Int. J. Electrochem. Sci., 12 **(2017)** 8535 – 8551, doi: 10.20964/2017.09.53

International Journal of ELECTROCHEMICAL SCIENCE
www.electrochemsci.org

The Efficiency of Eco-friendly Schiff Bases as Corrosion Inhibitor for Stainless Steel in Hydrochloric Acid Solution

Nathir A. F. Al-Rawashdeh[1,*], *Ahmed S. Alshamsi*[2], *Soleiman Hisaindee*[2], *John Graham*[3], *Noura Al Shamisi*[2]

[1] Chemistry Department, Jordan University of Science & Technology, P.O. Box 3030, Irbid, Jordan
[2] Department of Chemistry, College of Science, United Arab Emirates University, Al-Ain, UAE
[3] Department of Environmental Science, Sligo Institute of Technology, Sligo, Ireland
[*]E-mail: nathir@just.edu.jo

Received: 19 May 2017 / *Accepted:* 12 July 2017 / *Published:* 13 August 2017

Six new Schiff bases, namely, ((E)-(Phenylimino)methyl)phenol (**1**), 2-((E)-(p-Tolylimino)methyl)phenol (**2**), (E)-2-(Hydroxybenzylideneamino)benzoic acid (**3**), (E)-2-(Hydroxybenzylideneamino)benzoic acid (**4**), 2-((E)-(2 Hydroxyphenylimino)methyl) phenol (**5**), and 2-((E)-(2 Mercaptophenylimino)methyl)phenol (**6**) were synthesized and fully characterized. The inhibition efficiencies on the corrosion of stainless steel (304SS) in hydrochloric acid solution were investigated by weight loss, cyclic polarization, and polarization resistance methods. The quantum chemical calculations were performed to provide further insight into the inhibition efficiencies that determined experimentally. Also, the surface morphology of few sample were analyzed by Atomic force microscopy (AFM). The results indicated that inhibition efficiency (I%) increased with increasing inhibitor concentration and decreasing the corrosive media concentration. The effectiveness of the tested inhibitors increased in the order of **1**<**4**<**2**<**3**<**5**<**6**, and mainly depends on the adsorption behavior and molecular structure of the inhibitor.

Keywords: Schiff bases; stainless steel; weight loss; polarization; acid corrosion

1. INTRODUCTION

Stainless steel widely used for food handling and cutlery among many other applications, and has been used extensively in the chemical, refrigeration, paper and food processing industries because of its relatively good corrosion resistance and high availability. In the presence of oxygen, a passive film layer of chromium-rich oxide formed on the surface of stainless steel, which makes it highly resistive to corrosion in normal atmospheric conditions [1-3]. However, this layer could be damaged in harsh environments. Therefore, corrosion inhibitors are added to decrease the rate at which this layer is

removed in different media. Stainless steels have good corrosion resistance in oxidizing acid media; however, they are easy to be corded in reducing acids such as sulfuric acid (H_2SO_4) and hydrochloric acid (HCl) [4-8].

In many industries, the challenging problem of using stainless steel is its dissolution in acidic medium where hydrochloric acid (HCl) is widely used as pickling acid for steel and for other applications such as, acid cleaning, acid descaling, and oil well acidizing. Therefore, the corrosion inhibition of stainless steel in HCl medium has been comprehensively investigated in the field of engineering, chemical and electrochemical industries, and power production [1-8]. Several organic compounds and environmentally safe corrosion control agent have been reported as corrosion inhibitors for steel [1-13]. However; the corrosion efficiency generally was very low. There are many factors affecting the extent of adsorption of an inhibitor, of these, the nature and the surface charge of the metal, the mode of adsorption of the inhibitor, the inhibitor's chemical structure, and the type of the aggressive solution. Also, the adsorption of inhibitors on surface of metal could be enhance in the presence of heteroatoms (such as: oxygen, nitrogen, sulfur, phosphorus) and aromatic rings in the inhibitor's chemical structure [14-16].

Schiff bases have many applications and uses in biochemistry and chemistry due to the ease of their synthesis from relatively inexpensive starting materials and were classified as eco-friendly or low toxic properties [17]. Recently, Schiff bases have been recently identified as corrosion inhibitors for carbon steel, other metals, and alloys in acidic media [18-21]. Schiff bases have a unique chemical structure which is the presence of imine group (R_1-C=N-R_2), highly electronegative atoms such as: nitrogen, sulfur, and/or oxygen, and π-electrons, which enhance their adsorption ability on a metal surface and showed high corrosion inhibition efficiency [19]. Asan [22] investigated the action mechanism of these types of corrosion inhibitors and found that these molecules normally form very thin films that reduce the corrosion rate by slowing down of anodic, cathodic reaction or both. Also, the inhibition efficiency of inhibitor depends on its structure, which includes the number of adsorption active centers in the molecule and their charge densities, the molecule size, and the mode of adsorption [23, 24].

It is well known that the molecular structure of compounds has a crucial effect on their chemical reactivity; hence it has been object of great interest in several disciplines of chemistry. Therefore, quantum chemical calculations have been widely used to investigate the electronic structure of molecule to support the results that obtained experimentally. The inhibition property of organic compounds has been often correlated with molecular properties. Therefore, it is worthwhile to compute these features theoretically [25].

In the present study, the inhibition efficiency of six new synthesized Schiff bases, namely *((E)-(Phenylimino)methyl)phenol* (**1**), *2-((E)-(p-Tolylimino)methyl)phenol* (**2**), (*E)-2-(Hydroxybenzylideneamino)benzoic acid* (**3**), *(E)-2-(Hydroxybenzylideneamino)benzoic acid* (**4**), *2-((E)-(2-Hydroxyphenylimino)methyl)phenol* (**5**), and *2-((E)-(2 Mercaptophenylimino)methyl)phenol* (**6**), on the corrosion of stainless steel (304SS) in hydrochloric acid solution at room temperature has been reported. Weight loss method, cyclic polarization technique, and quantum chemical calculations method were used to investigate the inhibition efficiency of these Schiff bases. Also, the surface morphology of few sample were tested by Atomic force microscopy (AFM).

2. EXPERIMENTAL

2.1. Materials

Stainless steel sheets (304SS) of composition (0.08% C, 2.0% Mn, 0.045% P, 0.030% S, 0.75% Si, 19% Cr, 11% Ni and balance Fe) and 0.05 cm thickness, supplied by Alfa Aesar, were used in the study. The sheets were mechanically press cut into 3×1 cm coupons. These coupons were used as cut with further polishing. However, they were degreased in acetone and rinsed with ether prior to their use in corrosion studies. For polarization measurements 304SS wire of 1 mm in diameter, supplied by Alfa Aesar, was tested as received in 0.1 M HCl as a function of Schiff base at room temperature (~22 °C). The concentrations of hydrochloric acid (HCl) prepared and used in the study were 0.1, 0.5, and 1.0 M. Reagent grade solvents and chemicals were purchased from Sigma Aldrich and were used without further purification.

2.2. Methods

2.2.1. Preparation of the Schiff bases

Melting points are reported as uncorrected. All Infrared (IR) spectra were recorded from samples on KBr disk. ^{1}H NMR and ^{13}C NMR spectra were recorded on Varian NMR spectrometers at 400 and 100 MHz respectively. The proton chemical shifts were reported in parts per million (δ ppm) and coupling constants (J) in Hertz (Hz) and s, d, t, m, br s refer to singlet, doublet, triplet, multiplet and broad singlet, respectively. All the Schiff bases (**1-6**) were prepared according to the general procedure for the synthesis of Schiff base (**1**), and the chemical structure were shown in Figure 1.

*((E)-(Phenylimino)methyl)phenol (**1**)*

A stirred mixture of salicylaldehyde (1.22g, 10 mmol) and aniline (837 mg, 9 mmol) in bench ethanol (10 mL) was refluxed for 3 h. The mixture was cooled in an ice-bath and the resulting yellow crystals were filtered, washed with cold ethanol and dried under vacuum to give **1** (650 mg,37%); mp: 44-45 °C; IR (cm^{-1}): 3418, 1622,1592; ^{1}H NMR (400 MHz, DMSO-d_6): δ = 6.92-6.97 (m, 2H), 7.25-7.30 (m, 1H), 7.36-7.45 (m, 5H), 7.61-7.64 (m, 1H), 8.91 (s, 1H), 13.15 (s, 1H); ^{13}C NMR (100 MHz, DMSO-d_6): δ = 117.0, 119.5, 119.7, 121.8, 127.4, 129.9, 133.1, 133.7, 148.5, 160.8, 163.9; exact mass *m*/*z* calcd for $C_{13}H_{11}NO$ 197.08406, found 198.09164 (M+H).

*2-((E)-(p-Tolylimino)methyl)phenol (**2**)*

Salicylaldehyde (1.22g, 10 mmol) and 4-methylaniline (965mg, 9 mmol) were used to prepare **2** (1.38 g, 72%) according to the general procedure; mp: 95-96 °C; IR (cm^{-1}): 3455, 1619, 1589, 1498; ^{1}H NMR (400 MHz, DMSO-d_6): δ = 2.24 (s, 3H), 6.91-6.95 (m, 2H), 7.19-7.21 (m, 2H), 7.26-7.29 (m, 2H), 7.37 (dd, J_{AB}= 15.6 Hz, J_{AX}=2.0 Hz, 1H), 7.36-7.37 (m, 1H), 7.59 (dd, J_{AB}= 8.0 Hz, J_{AX}=

2Hz, 1H), 8.89 (s, 1H), 13.2 (s br, 1H); ^{13}C NMR (100 MHz, DMSO-d_6): δ 21.0, 117.0, 119.5, 119.7, 121.6, 130.3, 132.9, 133.4, 136.9, 145.8, 160.8, 162.9; exact mass *m*/*z* calcd for $C_{14}H_{13}NO$ 211.09971, found 212. 10679, (M+H).

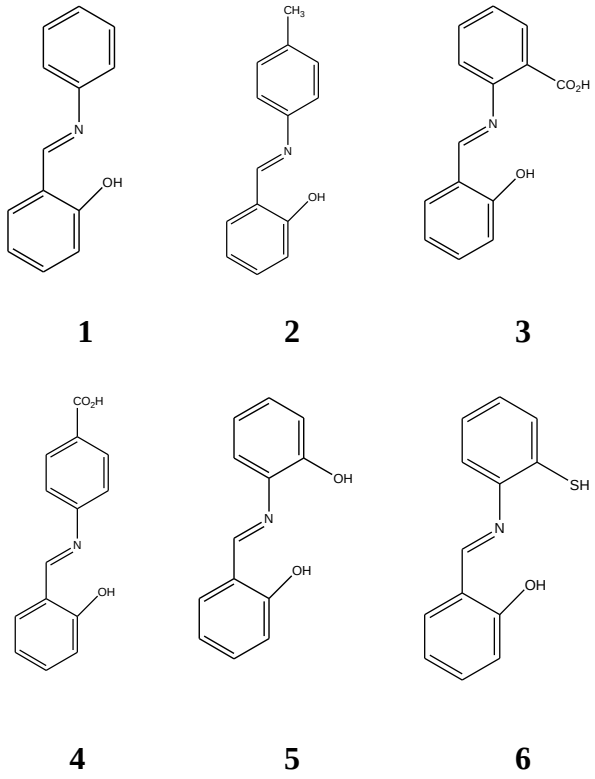

1 **2** **3**

4 **5** **6**

Figure 1. Chemical structure of Schiff bases.

*(E)-2-(Hydroxybenzylideneamino)benzoic acid (**3**)*

Salicylaldehyde (1.22 g, 10 mmol) and 2-aminobenzoic acid (1.23 g, 9 mmol) were used to prepare **3** (1.42 g, 65%) according to the general procedure; IR (cm^{-1}): 3413, 3069, 2952, 1682, 1619, 1569; ^{1}H NMR (400 MHz, DMSO-d_6): δ = 6.91-6.96 (m, 2H), 7.30-7.45 (m, 3H)), 7.62-7.60 (m, 2H), 7.84 (d, J=6.8 Hz, 1H), 8.83 (s br, 1H), 13.00 (s br, 2H); ^{13}C NMR (100 MHz, DMSO-d_6): δ = 110.0, 115.0, 116.7, 117.6, 119.5, 119.9, 122.7, 129.7, 131.6, 134.2, 136.8, 151.9, 161.2, 170.0; exact mass *m*/*z* calcd for $C_{14}H_{11}NO_3$ 241.07389, found 242.08575 (M+H).

2-((E)-(2-Hydroxybenzylideneamino)methyl)benzoic acid (4)

Salicylaldehyde (1.22g, 10 mmol) and 4-aminobenzoic acid (1.23 g, 9 mmol) wree used to prepare **4** (1.62 g, 74%) according to the general procedure; IR (cm^{-1}): 3467, 1620, 1600, 1569; ^{1}H NMR (400 MHz, DMSO-d_6): δ = 6.94-6.99 (m, 2H)7.39-7.47 (m , 3H), 7.65-7.68 (m, 1H), 7.97-8.00 (m, 2H), 8.96 (s, 1H), 12.65 (s br , 1H), 12.90 (s br , 1H); ^{13}C NMR (100 MHz, DMSO-d_6): δ 117.1, 119.8, 122.0, 129.2, 131.2, 133.1, 134.3, 152.6, 160.8, 165.2, 167.3; exact mass *m*/*z* calcd for $C_{14}H_{11}NO_3$ 241.07389, found 242.08577 (M+H).

*2-((E)-(2-Hydroxyphenylimino)methyl)phenol **(5)***

Salicylaldehyde (1.22g, 10 mmol) and 2-aminophenol (982 mg, 9 mmol) were used to prepare **5** (1.63 g, 85%) according to the general procedure; IR (cm^{-1}): 3467, 1619; ^1H NMR (400 MHz, DMSO-d_6): δ = 6.83-6.97 (m, 4H), 7.06-7.13 (m, 1H), 7.32-7.38 (m, 2H), 7.58 (dd, J_{AB}= 8.0 Hz, J_{AX}=1.6 Hz, 1H), 8.94 (s, 1H), 9.72 (s br , 1H), 13.80 (s br, 1H); ^{13}C NMR (100 MHz, DMSO-d_6): δ 117.0, 117.1, 119.1, 119.9, 120.03, 120.06, 128.5, 132.8, 133.3, 135.4, 151.6, 161.2, 162.1; exact mass *m/z* calcd for $C_{13}H_{11}NO_2$ 213.07898, found 214.09009 (M+H).

*2-((E)-(2-Mercaptophenylimino)methyl)phenol (**6**)*

Salicylaldehyde (1.22 g, 10 mmol) and 2-aminothiophenol (1.13 g, 9 mmol) were used to prepare **6** (1.90 g, 92%) according to the general procedure; Yield: 1.90 g (92%); IR (cm^{-1}): 3469, 3255, 1617, 1584; ^1H NMR (400 MHz, DMSO-d_6): δ = 6.49 (d, *J* = 2.4 Hz, 1H), 6.53-6.57 (m, 1H), 6.66 (d, *J* = 7.6Hz, 1H), 6.75-6.87 (m, 4H), 6.93 (d, *J* = 7.6Hz, 1H), 7.06-7.11 (m, 1H), 7.39 (d, *J* = 6.4 Hz, 1H), 9.89 (s, 1H); ^{13}C NMR (100 MHz, DMSO-d_6): δ = 109.0, 115.3, 118.9, 119.2, 121.6, 125.6, 126.3, 129.0, 130.0, 148.3, 153.9; exact mass m/z calcd for $C_{13}H_{11}NOS$ 229.29750, found 230.30910 (M+H).

2.2.2. Weight loss measurement

In the weight loss experiments, the pre-cleaned stainless steel coupons were suspended in test tubes containing 15 ml of test solutions maintained at 25 °C in a thermo stated bath. The weight loss was determined by retrieving the coupons for 24 h, washed with distilled water cleaned with bristle brush, rinsed with acetone, dried and reweighed. The weight loss was taken to be the difference between the weight at a given time and the original weight of the coupons. The measurements were carried out for the uninhibited solution (blank). Triplicate determinations were carried out. The corrosion rate (CR) was computed using equation 1.

$$Corrosion\ rate\quad (CR) = \frac{m_1 - m_2}{At} \qquad (1)$$

Where, m_1 and m_2 are the weight loses (mg) before and after immersion in the test solutions, respectively, *A* is the surface area of the specimens (cm^2) and *t* is the exposure time (hour).

The inhibition efficiency (I%) of Schiff bases was evaluated using the following equation:

$$I\% = \left(\frac{CR_{blank} - CR_{inh}}{CR_{blank}} \right) x100\% \qquad (2)$$

Where, CR_{blank} and CR_{inh} are the corrosion rate in the absence and presence of the inhibitor, respectively.

2.2.3. Polarization measurements

The 304SS steel wire, 1 mm in diameter, was coated with epoxy leaving the cross sectional area ($7.85x10^{-3}$ cm^2) exposed to the testing solution. Prior to each experiment the sample was wet-

ground using 240 to 600 grit SiC papers, cleaned with distilled water, and placed in a 3-electrode cell with Pt used as a counter electrode and saturated Ag/AgCl electrode, (+197 mV vs. standard hydrogen electrode). Standard corrosion techniques that have been employed include polarization resistance (R_p) versus time measurements and cyclic polarizations measurements. Cyclic polarization measurements were conducted using a scanning rate of 1.0 mV/s with the scans initiated at -500 mV, scanned to +400 mV or until a threshold current density of 100 mA/cm^2 is reached, and then reversed to -500 mV. The *Rp vs. time* measurements were conducted using a scanning rate of 0.1 mV/s with experiments conducted within ± 10 mV vs. Ec. Three measurements were collected per experiment with 800 s time interval between measurements. Data were collected automatically with the aid of a potentiostat/galvanstat (Gamry G750). All data analysis and extrapolations were performed using Gamry corrosion software (Gamry Echem Analyst). Magnetic stirrer with a constant rate was maintained in all experiments. An average of three independent experiments was conducted for a given set of conditions in order to verify the results. The open circuit potential was monitored for 30 minutes prior to starting the polarization experiment.

2.2.4. Quantum chemical calculation

All calculations were performed using Gaussian 09w rev. A01. All structures were optimized in the gas phase using the B3LYP hybrid functional and 6-311+G(d,p) basis set. Energy minima were confirmed by vibrational frequency calculations. The PCM model was used to simulate solvent effects on orbital energies using the gas-phase optimized geometries.

2.2.5. Atomic force microscopy

The surface morphology of the stainless steel (304SS) specimens was examined after polishing and after exposure to 1.0 M hydrochloric acid in the absence and presence of optimal concentration of the inhibitor, Schiff base **6** (1x10^{-3} M), using Flex-Anxiom — AFM for materials research (Nanosurf AG-Switzerland)

3. RESULTS AND DISCUSSION

3.1. Weight loss measurements

The weight loss measurements results for the corrosion of stainless steel sheets (304SS) in presence and absence of different concentrations of Schiff bases (**1-6**) in 0.1, 0.5, and 1.0 M HCl at 25 °C were summarized in Table 1 and shown in Figure 2. The corrosion rate (CR) was computed using equation 1 and the inhibition efficiency (I%) of Schiff bases was evaluated using equation 2. Table 1 show that the weight loss of stainless steel increases as the concentration of hydrochloric acid increases, and decreases as the concentration of the inhibitor (Schiff bases) increases. The inhibition efficiency (I%) of the tested Schiff bases in different concentration of HCl increased in the following

order: **1**<**4**<**2**<**3**<**5**<**6** (Table 1). Fouda [26] found that the extent of percentage inhibition depends on the molecular size and electron density on the active groups and atoms. The high inhibition efficiencies of tested Schiff bases towards stainless steel is due to the presence of azomethine (–C=N-) group, an electron cloud on the aromatic ring and presence of nitrogen, oxygen and sulphur atoms in the molecules [26]. The Schiff bases are strongly adsorbed via the donation of the lone pair of electrons of O atom in the carbonyl group and S atom in the C-S group and N atoms to metal surface [26]. The results were consistent with a previous study by Naik and Shah [21], for efficiency of Schiff bases as corrosion inhibitors for Aluminium in acidic media. In their study, the effect of the position of functional group on Schiff bases on corrosion inhibition was investigated [21]. Figure 2 show that the corrosion rates (CR) of stainless steel in hydrochloric acid decreased with increasing the concentration of Schiff bases (SB) until reached the optimal concentration value of 1.0 mM for SB. Also it shows an increase in the corrosion rate with increasing acid concentration, and the corrosion rate was reduced in the presence of all tested Schiff bases (**1-6**) compared to the blank corrosion in HCl. This indicates that the solution of Schiff bases inhibits the corrosion of stainless steel in acidic medium and the extent of corrosion inhibition (Table 1) depends on the amount of the SB and the concentration of hydrochloric acid Figure 2 (A-C). Figure 2 reveals that an increase in the concentration of tested Schiff bases decreased the corrosion rate and hence the corrosion inhibition efficiency increased (Table 1). The inhibition efficiency increases with increasing the SB concentration mainly due to the adsorption of the SB on the steel metal surface. The adsorption of SB on the stainless steel surface makes a barrier for mass and charge transfer. Consequently, the metal is protected from the aggressive anions of the acid. However, the presence of chloride ions from the hydrochloric acid in solution containing SB play a significant role in the adsorption process that results from increased surface coverage as a result of ion-pair interactions between the positively charged protonated Schiff bases and the chloride ions in acidic solution, which facilitates adsorption on the metal surface through a coordinate type of linkage. The complete protonation of Schiff bases by strong acids such as HCl is defined by the following equation [27]:

$$R_1\text{-}CH=N\text{-}R_2 + HCl \rightarrow [R_1\text{-}CH=N + H\text{-}R_2]Cl$$

3.2. Polarization measurements

The electrochemical parameters namely corrosion potential (E_{corr}), corrosion current density (i_{corr}), and pitting potential (E_{pit}) obtained from cyclic polarization curves and the results that derived from polarization resistance measurements of 304SS for $1x10^{-3}$ M Schiff bases (**1-6**) in 0.1 M HCl at 22 °C were summarized in Table 2 and 3, respectively. The inhibition efficiency (I%) was calculated using the equations 3 and 4.

$$I\% = \left[\frac{R_{p(i)} - R_p}{R_{p(i)}}\right] x100\% \quad (3)$$

$$I\% = \left[\frac{i_{corr} - i_{cor(i)}}{i_{corr}}\right] x100\% \quad (4)$$

R_p and $R_{p(i)}$ are the polarization resistance in the absence and in the presence of Schiff base, respectively. i_{corr} and $i_{corr(i)}$ are the corrosion current density in the absence and presence of Schiff base, respectively. Results summarized in Table 2 and 3, reveals that the best inhibitors of the tested Schiff bases were **6** and **5**. These two Schiff bases have very similar chemical structures as shown in Figure 1, and it seems that the functional group –SH has higher affinity to be adsorbed on the steel surface than –OH group, therefore **6** has high inhibition efficiency than **5** (Table 2 and 3).

Table 1. Weight loss (WL, mg)[a] and Inhibition efficiency (I%) of Schiff bases (SB) (**1**-**6**) for stainless steel (304SS) in HCl

Schiff base	[SB] (mM)	WL (mg) (0.1 M)	WL (mg) (0.5 M)	WL (mg) (1.0 M)	I% (0.1 M)	I% (0.5 M)	I% (1.0 M)
6	0	98.56	127.34	340.78	-	-	-
	0.01	0.96	1.89	9.01	99.03	98.52	97.36
	0.05	0.85	1.78	7.58	99.14	98.60	97.78
	0.1	0.73	1.58	6.01	99.26	98.768	98.24
	0.5	0.65	1.46	4.03	99.35	98.85	98.82
	1.0	0.49	1.23	3.79	99.50	99.03	98.89
5	0	98.56	127.34	340.78	-	-	-
	0.01	0.98	2.05	10.12	99.00	98.39	97.03
	0.05	0.91	1.91	9.82	99.08	98.50	97.12
	0.1	0.81	1.74	8.58	99.18	98.63	97.48
	0.5	0.74	1.53	7.63	99.25	98.80	97.76
	1.0	0.69	1.24	6.08	99.30	99.03	98.22
4	0	98.56	127.34	340.78	-	-	-
	0.01	10.19	15.04	41.17	89.66	88.19	87.92
	0.05	9.78	13.12	38.11	90.08	89.70	88.82
	0.1	8.35	11.43	31.05	91.53	91.02	90.89
	0.5	7.13	10.21	29.92	92.77	91.98	91.22
	1.0	6.8	9.01	28.17	93.10	92.92	91.73
3	0	98.56	127.34	340.78	-	-	-
	0.01	3.01	5.02	14.43	96.95	96.06	95.77
	0.05	2.94	4.73	13.42	97.02	96.29	96.06
	0.1	2.81	4.05	11.96	97.15	96.829	96.49
	0.5	2.67	3.82	11.05	97.29	97.00	96.76
	1.0	2.56	3.61	10.03	97.40	97.17	97.06
2	0	98.56	127.34	340.78	-	-	-
	0.01	8.67	11	31.14	91.20	91.36	90.86
	0.05	7.04	9.93	27.67	92.86	92.20	91.88
	0.1	6.32	8.79	24.31	93.59	93.10	92.87
	0.5	5.91	8.03	23.72	94.00	93.70	93.04
	1.0	5.62	7.51	20.65	94.30	94.10	93.94
1	0	98.56	127.34	340.78	-	-	-
	0.01	11.65	17.06	50.18	88.18	86.60	85.27
	0.05	10.21	15.82	47.07	89.648	87.58	86.19
	0.1	8.93	13.78	39.04	90.94	89.18	88.54
	0.5	8.01	12.04	33.83	91.87	90.54	90.07
	1.0	7.4	11.37	31.07	92.49	91.07	90.88

[a]Average triplicate determinations were carried out. Standard deviation (SD) in the range of 0.01-0.10.

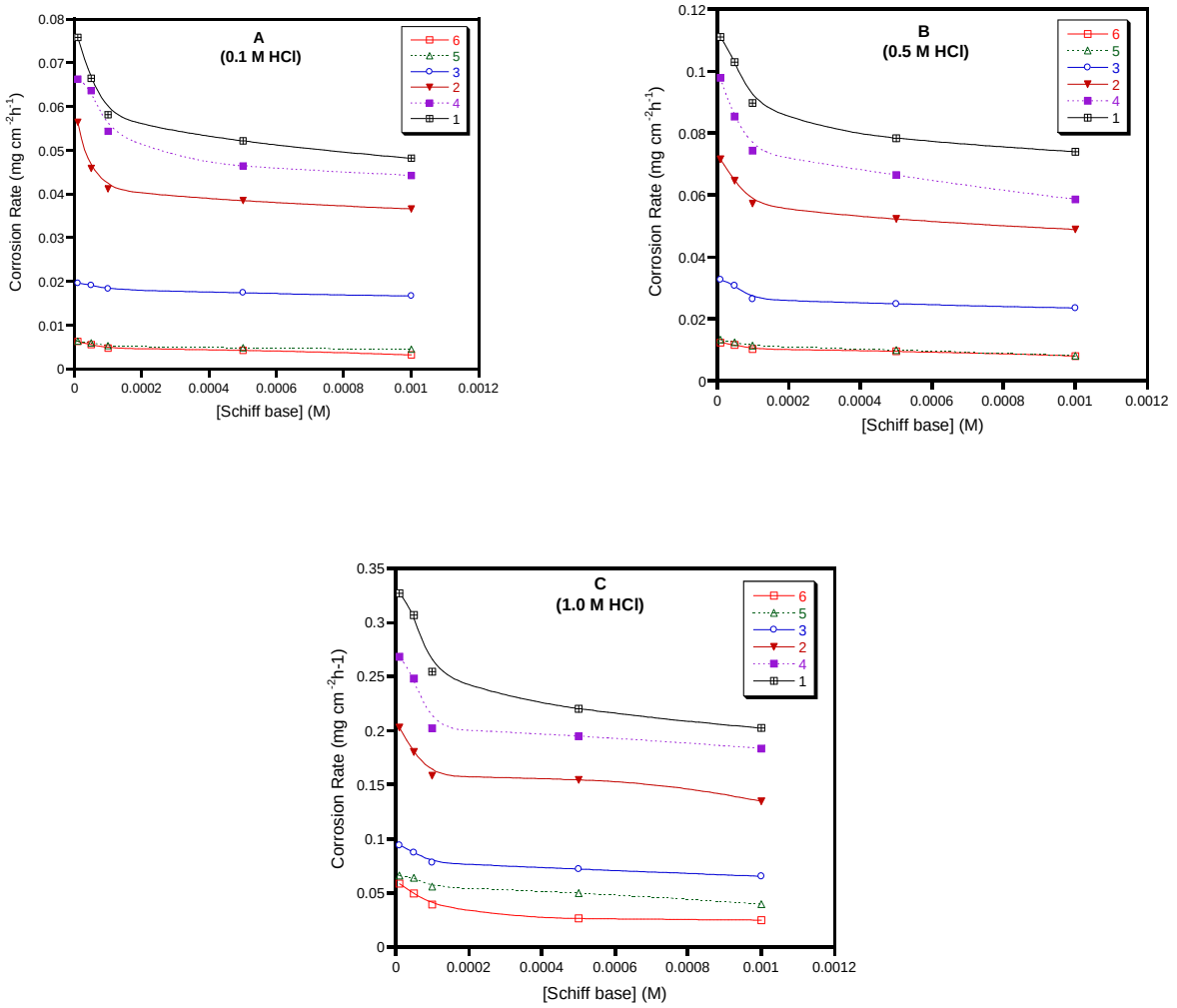

Figure 2. Corrosion rate at different concentration of Schiff bases for stainless steel sheets (304SS) from weight loss measurements at 25 °C in (**A**) 0.1 M HCl, (**B**) 0.5 M HCl, and (**C**) 1.0 M HCl.

Table 2. Data extrapolated from cyclic polarization curves of 304SS for $1x10^{-3}$ M Schiff bases (**1-6**) in 0.1 M HCl at 22 ^{o}C

Schiff Base	E_{corr} (mV *vs.* Ag/AgCl, sat.)	i_{corr} (A/cm^2)	E_{pit} (mV)	*I%*
0.1 M HCl	-346	$9.020x10^{-3}$	266	-
6	-328	$2.760x10^{-5}$	392	99.69
5	-341	$4.650x10^{-5}$	390	99.49
4	-353	$5.322x10^{-4}$	381	94.10
3	-348	$1.524x10^{-4}$	386	98.31
2	-350	$4.375x10^{-4}$	384	95.15
1	-358	$6.260x10^{-4}$	376	93.06

Table 3. Polarization resistance data, of 304SS for $1x10^{-3}$ M Schiff bases (**1**-**6**) in 0.1 M HCl at 22 °C

Schiff Base	*Rp* (Ω-cm^2, from Rp vs. t)	*I%* (from Rp vs. t)	*Rp* (Ω-cm^2, from cyclic polarization)	*I%* (from cyclic polarization)
0.1 M HCl	493	-	16.62	-
6	$1.736x10^4$	97.16	2441	99.32
5	$1.627x10^4$	96.97	1933	99.14
4	$6.828x10^3$	92.78	266.4	93.76
3	$1.347x10^4$	96.34	839.5	98.02
2	$7.665x10^3$	93.57	330.3	94.97
1	$5.502x10^3$	91.04	234.1	92.90

This result is consistent with what has been observed for adsorption capacity of sulfur atom compared to oxygen atom over metal surfaces [28-30]. As reported in literature [28-30], it has been found that the adsorption capacities of heteroatom present in the organic inhibitor molecules is in the order O<N<S<P. In this study, the inhibition efficiency (I%) of the tested Schiff bases in 0.1 M HCl increased in the following order: **1**<**4**<**2**<**3**<**5**<**6** (Table 2 and 3). This result is consistent with the order of adsorption capacities of heteroatom present on the tested Schiff bases [28-30]. The inhibition mechanism of Schiff bases has been investigated by Patel [18], where they found that the Schiff base molecule will lie flat on the metal surface and covers the adjoining positions of the surface [18].

To test the effect of Schiff bases concentration on corrosion inhibition efficiency of stainless steel, a cyclic polarization and polarization resistance measurements of 304SS for Schiff base (**6**) in 0.1 M HCl at 22 °C were reported. The cyclic polarization curves for stainless steel sheets (304SS) in presence and absence of different concentrations of Schiff base (**6**) in 0.1 M HCl at 22 °C were shown in Figure 3 (A-F), and the obtained electrochemical parameters were summarized in Table 4. Furthermore, the results that derived from polarization resistance measurements at different concentrations of Schiff base (**6**) in 0.1 M HCl at 22 °C were summarized in Table 5. Examination of the cyclic polarization curves in HCl solution in absence of Schiff bases (Figure 3 A) reveals that the polarization curves exhibit active dissolution without transition to passivation within the range of studied potential, while in the presence of Schiff bases (Figure 3 B-F, at different concentration of **6**) the passive current density decreases as the passivity range increases with increasing Schiff base concentration. These results supported with the fact that the addition of Schiff base has a little effect on the value of corrosion potential (E_{corr}) (Table 4). Table 2 and 4, show that the corrosion current (i_{corr}) in 0.1 M HCl is very high in absence of Schiff bases. This indicates strong corrosiveness of stainless steel in acidic media, due to the fact that a strong acid such as HCl has a good electrical conductivity as well as high rate of ion migration [31].

The corrosion current (i_{corr}) remarkably dropped in the presence of Schiff bases (Table 2) and the extent of reduction is found to be concentration dependent (Table 4), as the concentration of Schiff base increases the corrosion current decreases, and the lowest value was obtained at $1x10^{-3}$ M of Schiff base in 0.1 M HCl. The magnitude of the critical current density decreases with increasing Schiff base

concentration with a value of about 5 mA/cm^2 in the absence of Schiff base to a minimum value of about a 100 nA/cm^2 in the presence of 1x10^{-3} M Schiff base (**6**). Table 2, shows that the pitting potential (E_{pit}) increases in the presence of Schiff bases, indicating Schiff base ability to enhance pitting corrosion resistance, and the extent of reduction is found to be concentration dependent (Table 4), as the concentration of Schiff base (**6**) increases the pitting potential increases, and the highest value was obtained at 1x10^{-3} M of Schiff base in 0.1 M HCl. Tables 4 and 5 show that the Schiff bases have a very good corrosion inhibition as both the polarization resistance (R_p) values increase with increasing concentration while i_{corr} values decrease with increasing concentration of Schiff base. The values of R_p obtained from the R_p *vs. time* curves (Figure 4) are much higher than those extrapolated from the cyclic polarization curves (Table 3 and 5); nevertheless, both increases as a function of Schiff base concentration. Table 5 shows that as the concentration of Schiff base (**6**) increases the corrosion inhibition efficiency (I%) increases and range of 95.42-99.32%. Furthermore, the inhibition efficiency (I%) of 304SS for 1x10^{-3} M Schiff bases (**1-6**) in 0.1 M HCl obtained from cyclic polarization curves and polarization resistance measurements (Table 2 and 3) are found to be in a good agreement with that obtained with the weight loss measurements (Table 1).

Table 4. Data extrapolated from cyclic polarization curves of 304SS in 0.1 M HCl at different concentration of Schiff base (**6**) at 22 °C

[Schiff base (6)] (M)	***E*$_{corr}$ (mV *vs*.Ag/AgCl, sat.)**	***i*$_{corr}$ (A/cm^2)**	***E*$_{pit}$ (mV)**	***I%***
Blank	-346	9.020x10^{-3}	266	-
1x10^{-5}	-358	8.810x10^{-5}	298	99.02
5x10^{-5}	-330	7.710x10^{-5}	325	99.14
1x10^{-4}	-345	6.320x10^{-5}	329	99.30
5x10^{-4}	-345	4.980x10^{-5}	392	99.45
1x10^{-3}	-328	2.760x10^{-5}	394	99.69

Table 5. Polarization resistance data of 304SS in 0.1 M HCl at different concentration of Schiff base (**6**) at 22 °C

[Schiff base (6)] (M)	***R*$_p$ (Ω-cm^2, from R$_p$ vs. t)**	***I%* (from R$_p$ vs. t)**	***R*$_p$ (Ω-cm^2, from cyclic polarization)**	***I%* (from cyclic polarization)**
Blank	493	-	16.62	-
1x10^{-5}	9.355x10^{+3}	94.73	362.8	95.42
5x10^{-5}	1.653x10^{+4}	97.02	727.1	97.71
1x10^{-4}	1.175x10^{+4}	95.80	1360	98.78
5x10^{-4}	1.736x10^{+4}	97.16	1569	98.94
1x10^{-3}	1.315x10^{+4}	96.25	2441	99.32

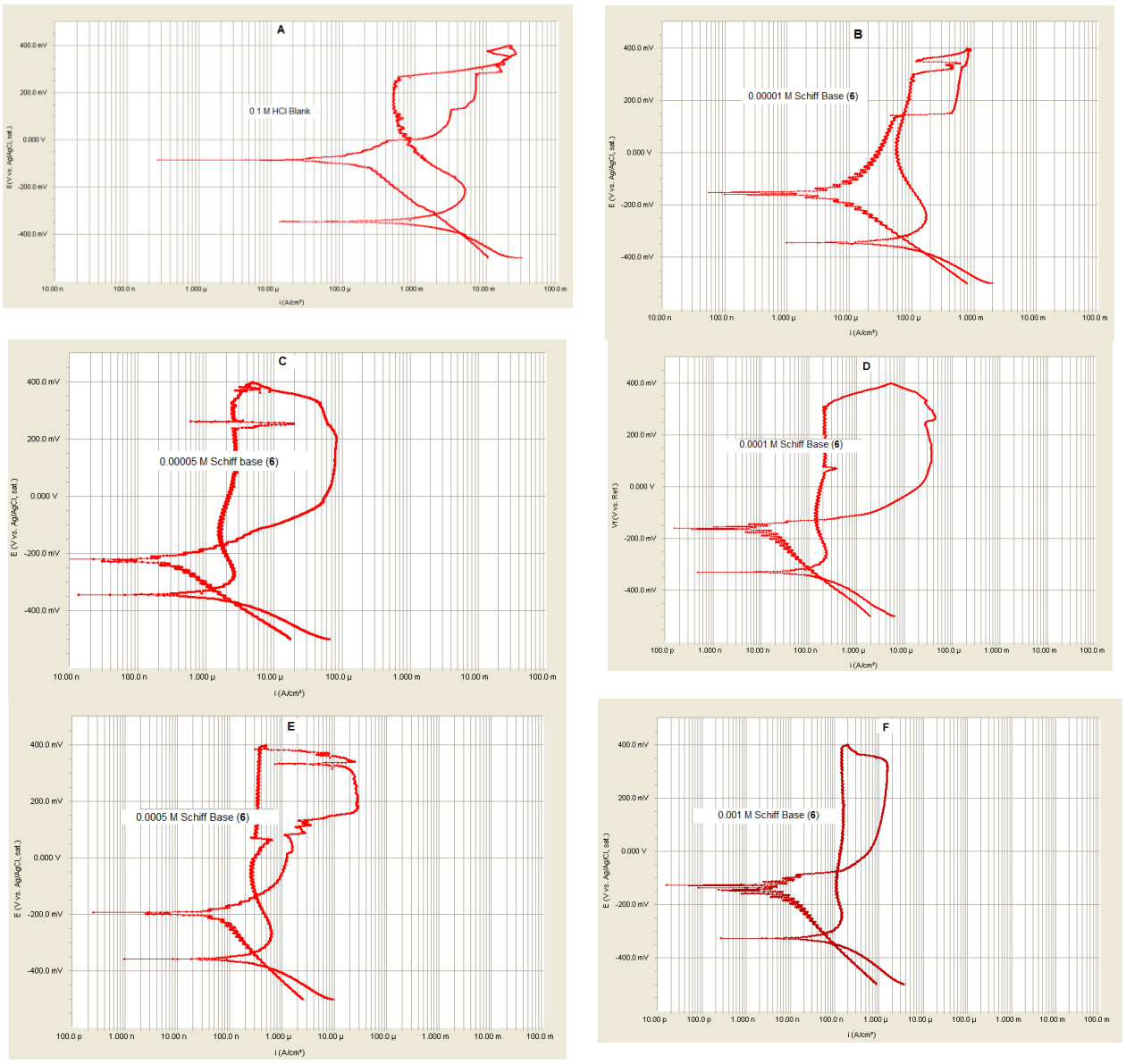

Figure 3. Cyclic polarization curves of 304SS in 0.1 M HCl at different concentration of Schiff base (**6**) at 22 °C. [SB] = 0 (**A**), 1x10^{-5} M (**B**), 5x10^{-5} M (**C**), 1x10^{-4} M (**D**), 5x10^{-4} M (**E**), 1x10^{-3} M (**F**).

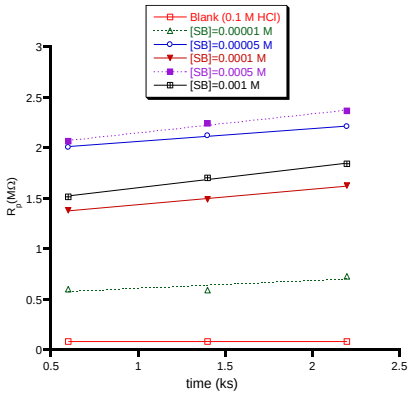

Figure 4. *Rp vs. time* of 304SS in 0.1 M HCl as a function of different concentration of Schiff base (**6**) at 22 °C.

3.3 Quantum chemical calculations

The quantum chemical calculations have been reported in many recent corrosion publications as a powerful tool for studying the mechanism of corrosion inhibition [19, 32-34]. It has been shown that the interactions between organic inhibitor and metal surfaces is related to some of the quantum chemical parameters such as the energy of the highest occupied molecular orbital (E_{HOMO}), the energy of the lowest unoccupied molecular orbital (E_{LUMO}), and the energy band gap ($\Delta E_{HL} = E_{HOMO}-E_{LUMO}$) [35, 36]. Thus, in this study the quantum chemical calculations were performed with complete optimization using Gaussian 09w rev. A01, to support the experimental results and investigate the inhibition effect of the tested Schiff bases. The electron donating ability of the molecule is represented by the value of E_{HOMO} while the ability of accepting electron represented by the value of E_{LUMO}. The higher the values of E_{HOMO} the higher the ability of the molecule to donate electrons to an acceptor molecule while the lower the value of E_{LUMO} implies the ease to accept electron by a molecule [37]. Therefore, an increase in E_{HOMO} (less negative) will enhance the adsorption and improve the inhibition efficiency. The reactivity tendency of a molecule towards the metal surface represents by the energy band gap, ΔE_{HL}. Since molecule with low energy gap is more polarizable and is generally associated with high chemical reactivity and low kinetic stability, therefore the reactivity of the molecule increases as ΔE_{HL} decreases, leading to an increase in adsorption of molecule onto a metal surface [35]. Thus, the lower the value of ΔE_H, the higher the inhibition efficiency of the adsorbed molecule [19]. In this study, the quantum chemical parameters E_{HOMO}, E_{LUMO}, and ΔE_{HL} in gas and aqueous phases were summarized in Table 6. The HOMO and LUMO of each Schiff base are π and π^* orbitals, respectively. As can be seen from data in Table 6, Schiff bases **6** has the highest value of E_{HOMO} (less negative) and the lowest value of ΔE_{HL} compared to other tested Schiff bases in this study. The values of the ΔE_{HL} of the six Schiff bases decreased in the following order: **1**>**4**>**2**>**3**>**5**,**6** (Table 6). This result is found to be in a good agreement with that obtained from the experimental measurements (weight loss, cyclic polarization curves and polarization resistance measurements) (Table 2-5), which implies that the Schiff bases **5** and **6** relatively have better corrosion performance than the other tested Schiff bases. Figure 5 shows a good correlations between the inhibition efficiency (I%) of Schiff bases (**1**-**6**) calculated by using weight loss, cyclic polarization, and polarization resistance methods with the Energy of HOMO-LUMO gap (ΔE_{HL}).

Table 6. The energies of the HOMO, LUMO, and HOMO-LUMO gap (HL gap) of Schiff bases (**1**-**6**) calculated in the gas phase and aqueous phase using Gaussian

Structure	E_{HOMO} gas phase (eV)	E_{LUMO} gas phase (eV)	ΔE_{HL} (gas) (eV)	E_{HOMO} (H_2O) (eV)	E_{LUMO} (H_2O) (eV)	ΔE_{HL} (H_2O) (eV)
1	-6.23	-2.09	4.14	-6.34	-2.12	4.21
2	-6.11	-2.02	4.09	-6.22	-2.09	4.13
3	-6.47	-2.51	3.96	-6.48	-2.46	4.01
4	-6.39	-2.28	4.11	-6.46	-2.28	4.18
5	-6.15	-2.31	3.84	-6.19	-2.25	3.95
6	-6.07	-2.25	3.82	-6.16	-2.20	3.95

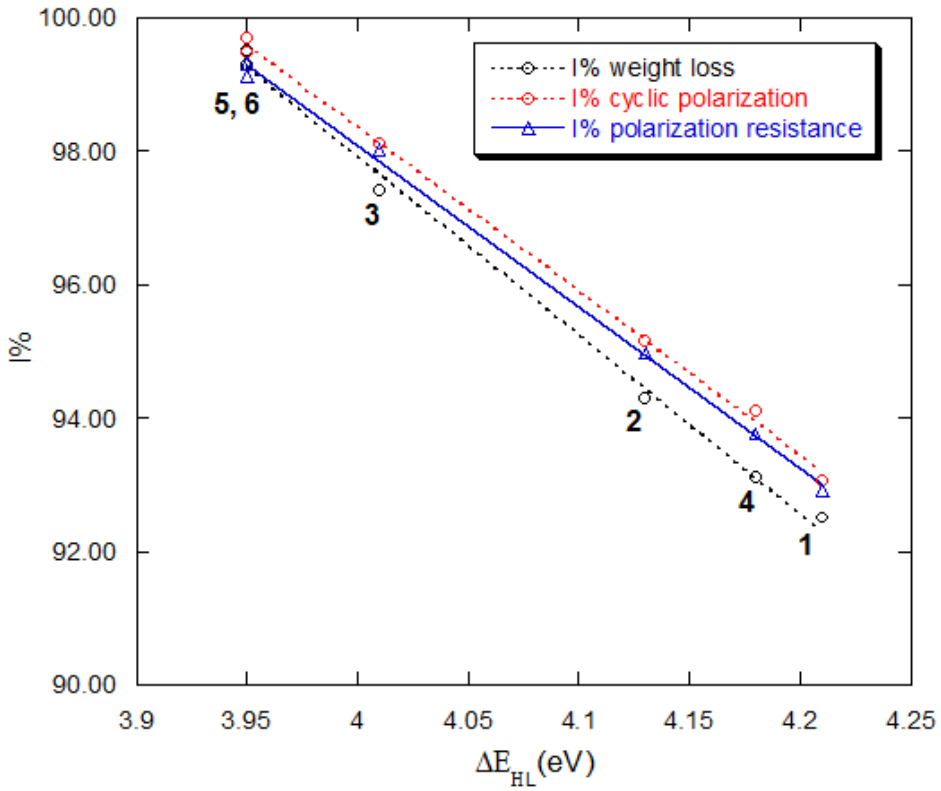

Figure 5. Inhibition efficiency (I%) of Schiff bases (**1-6**) calculated by using weight loss, cyclic polarization, and polarization resistance as function of Energy of HOMO-LUMO gap.

It is clear from Figure 5 that the inhibition efficiency (I%) increases as the ΔEHL of the Schiff bases decreases. Figure 5 is produced using the aqueous phase orbital energies - a similar relationship is found for gas-phase orbital energies (R^2 = 0.978). Neither the HOMO energy (EHOMO) nor LUMO energy (ELUMO) alone shows significant correlation with inhibition efficiency. Dipole moment does not correlate with inhibition efficiency either. Perhaps this implies that the mode of binding is analogous to that of low-valent metal complexes such as metal carbonyls and involves both donation and 'back-donation' between the ligand and the metal surface. The isosurfaces for the HOMO and LUMO of each Schiff base (**1-6**) were shown in Figure 6.

Schiff base	HOMO	LUMO
1	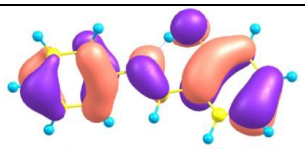	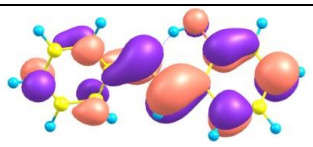
2	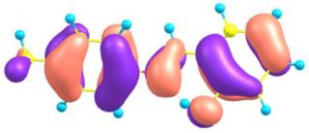	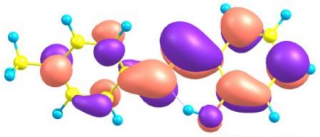
3	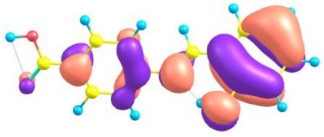	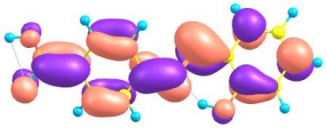

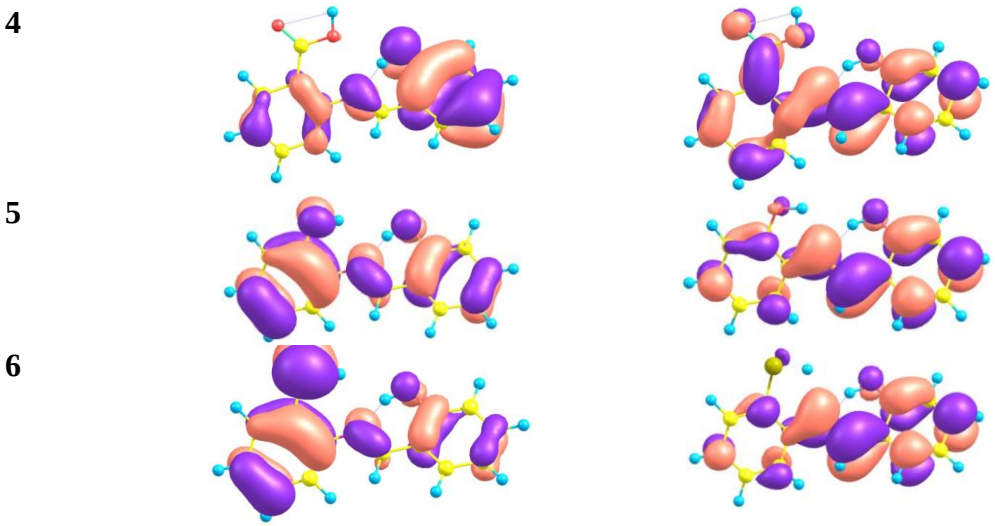

Figure 6. Isosurfaces for the HOMO and LUMO of Schiff bases (**1-6**).

3.4. Atomic force microscopy analysis

The surface roughness on a microscale of the stainless steel (304SS) specimens was examined after exposure to 1.0 M hydrochloric acid in the absence and presence of optimal concentration of the inhibitor, Schiff base **6** ($1x10^{-3}$ M). Figure 7 shows the AFM images of mild steel after 24 h exposure to 1.0 M HCl solution in the absence (Figure 7A) and presence of $1x10^{-3}$ M Schiff base **6** (Figure 7B and C). Figure 7A clearly reveals that the metal surface was strongly damaged in the absence of the inhibitor, due to metal dissolution in the corrosive acidic media. However, in the presence of Schiff base **6** (Figure 7B and C), the stainless steel surface roughness was significantly reduced, indicating the corrosion inhibition effect of the Schiff base.

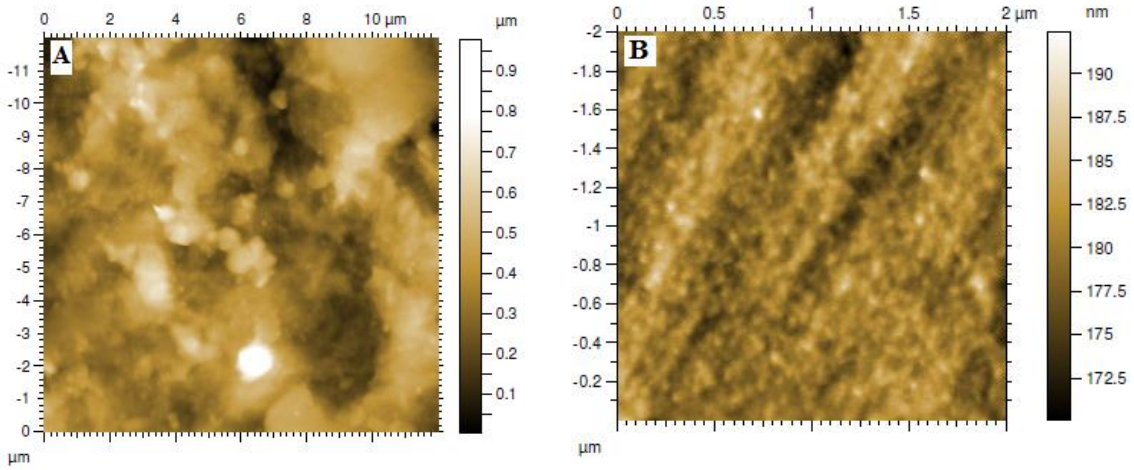

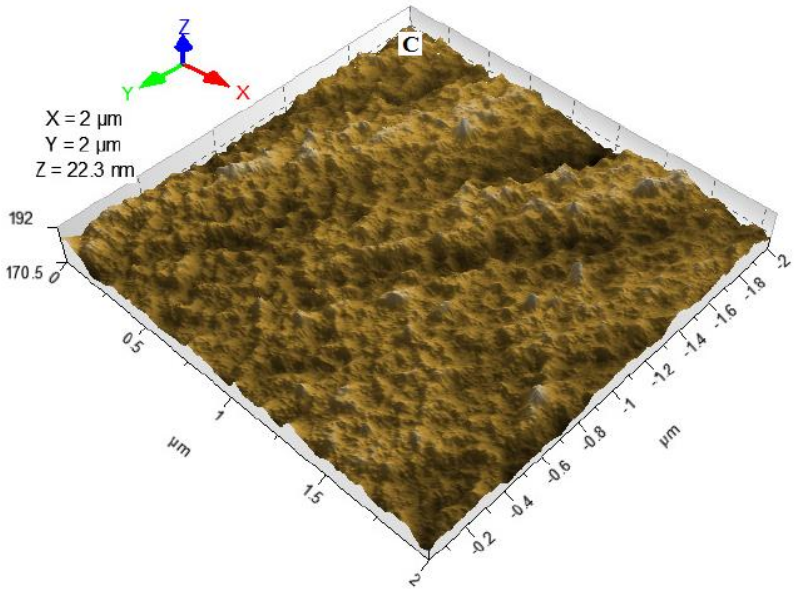

Figure 7. AFM images for exposed low stainless steel (**A**) in a 1.0 M HCl solution, (**B**) 1.0 M HCl with $1x10^{-3}$ M Schiff base **6,** (**C**) Three-dimensional AFM image of 1 M HCl with $1x10^{-3}$ M Schiff base **6.**

4. CONCLUSION

This study showed that the tested Schiff bases (**1-6**) were beneficial inhibitors for the corrosion of stainless steel (304SS) in acidic media. The inhibition efficiencies of the tested Schiff bases obtained from weight loss, cyclic polarization, and polarization resistance measurements are in good agreement with each other and showed that the ability of tested Schiff bases (**1-6**) as inhibitors increases in the order **1**<**4**<**2**<**3**<**5**<**6**. The differences in the inhibition efficiencies of the six tested Schiff bases may be due to the differences in their molecular structure, type of the functional groups, and the mode of adsorption. The inhibition efficiency (I%) increased with increasing inhibitor concentration and decreasing the corrosive media concentration. The quantum chemical calculations showed that the energy band gap ($\Delta E = E_{HOMO}-E_{LUMO}$) was correlated with the inhibition efficiencies obtained by weight loss, cyclic polarization, and polarization resistance methods and it was found that inhibition efficiency increased with lower ΔE_{HL} values and the higher E_{HOMO} (less negative). The values of the ΔE_{HL} of the six Schiff bases decreased in the following order: **1**>**4**>**2**>**3**>**5**,**6**. The AFM images confirm the protection of stainless steel in 1.0 M HCl solution by the tested Schiff bases. The cyclic polarization method showed that the E_{pitt} increases with increasing concentration of Schiff bases indicating the ability of Schiff bases to enhance pitting corrosion resistance. Furthermore, it showed that the passive current density decreases while the passivity range increases with increasing Schiff base concentration implies a very good corrosion inhibition for stainless steel corrosion.

ACKNOWLEDGMENTS
The authors acknowledge the financial support of the UAEU (Project No.: 31S014).

References

1. R. Loto, C. Loto and A. Popoola, *J. Mater. Environ. Sci.*, 3 (2012) 885.
2. J. H. Potgieter, F. V. Adams, N. Maledi, J. Van Der Merwe and P. A. Olubambi, *J. Chem. Mater. Sci.*, 2 (2012) 37.
3. M. Scendo and J. Trela, *Int. J. Electrochem. Sci.*, 8 (2013) 9201.
4. K. Varga, P. Baradlai, W. O. Barnard, G. Myburg, P. Halmosg and J. H. Potgieter, *Electrochim. Acta*, 42 (1997) 25.
5. R. Herle, P. Shetty, S. D. Shetty and U. A. Kini, Portugaliae, *Electrochim. Acta*, 29 (2011) 69.
6. P. Selvakumar, B. Karthik and C. Thangavelu, *Res. J. Chem. Sci.*, 3 (2013) 87.
7. M. Naghizadeh, D. Nakhaie, M. Zakeri and M. Moayed, *Corros. Sci.*, 94 (2015) 420.
8. R. T. Loto, C. A. Loto, A. P. Popoola and T. Fedotova, *Silicon*, 8 (2016) 145.
9. Y. Abboud, O. Tanane, A. El Bouari, R. Salghi, B. Hammouti, A. Chetouani and S. Jodeh, *Corros. Eng., Sci. Technol.*, 51(8) (2016) 557.
10. D. K. Yadav, M. A. Quraishi and B. Maiti, *Corros. Sci.*, 55 (2012) 254.
11. M. A. Abu-Dalo, A. A.Othman and N. A. F. Al-Rawashdeh, *Int. J. Electrochem. Sci.*, 7 (2012) 9303.
12. M. A. Abu-Dalo, N. A.F. Al-Rawashdeh and A. A. Mutlaq, *J. Iron Steel Res. Int.*, 23(7) (2016) 722.
13. M. A. Abu-Dalo, N. A. F. Al-Rawashdeh and A. Ababneh, *Desalination* , 313 (2013) 105.
14. O. L. Riggs, Jr., in C. C. Nathan (Ed.), *Corrosion Inhibitors*, NACE, (1973) Houston, TX.
15. I. Radojcic, K. Berkovic, S. Kovac and J. Vorkapic-Furac, *Corros. Sci.*, 50 (2008) 1498.
16. A. K. Maayta and N. A. F. Al- Rawashdeh, *Corros. Sci*., 46(5) (2004) 1129.
17. M. Lashgari, M. R. Arshadi and S. Miandari, *Electrochim. Acta*, 55 (2010) 6058.
18. A. S. Patel, V. A. Panchal and N. K. Shah, *Bull. Mater. Sci.*, 35(2) (2012) 283.
19. S. Safak, B. Duran, A. Yurt and G. Türkoglu, *Corros. Sci*., 54 (2012) 251.
20. M. Scendo and J. Trela, *Int. J. Electrochem. Sci.*, 8 (2013) 8329.
21. U. J. Naik and N. K. Shah, *Int. J. Innov. Res. Scoi. Eng. Technol*., 3(3) (2014) 10422.
22. A. Asan, M. Kabasakaloglu, M. Isıklan and Z. Kılıç, *Corros. Sci*., 47 (2005) 1534.
23. I. B. Obot, N. O. Obi-Egbedi and S. A. Umoren, *Corros. Sci*., 51 (2009) 1868.
24. P. C. Okafor and Y. Zheng, *Corros. Sci.*, 51 (2009) 850.
25. I. Ahamad, R. Prasad and M. A. Quraishi, *Mater. Chem. Phys*., 124 (2010) 1155.
26. A. S. Fouda, L. H. Madkour, A. A. El-Shafei and S. A. A. El Maksoud, *Bull. Korean .Chem. Soc.*, 16 (1995) 454.
27. D. Cossette and D. Vocell, *Can. J. Chem*., 65 (1987) 661.
28. B. D. C. Donnelly, T. C. Downie, R. Grzeskowiak, H. R. Hamburg and D. Short, *Corros. Sci.*, 18 (1977) 109.
29. A. B. Tadros and Y. Abdel-Naby, *J. Electroanal. Chem.*, 224 (1988) 443.
30. N. C. Subramanyam, B. S. Sheshadri and S. A. Mayanna, *Corros. Sci.*, 34 (1993) 563.
31. X. Li and S. Deng, *Corros. Sci*., 65 (2012) 299.
32. I. B. Obot and N. O. Obi-Egbedi, *Colloids Surf. A*, 330 (2008) 207.
33. G. Gece, *Corros. Sci*., 50 (2008) 2981.
34. S. A. Umoren, I. B. Obot and Z. M. Gasem, *Ionics*, 21 (2015) 1171.
35. M. K. Awad, M. R. Mustafa and M. M. Abo Elnga, *J. Mol. Struct. (THEOCHEM)*, 959 (2010) 66.
36. K. F. Khaled, *Corros. Sci*., 52 (2010) 2905.
37. M. M. Kabanda, I. B. Obot and E. E. Ebenso EE, *Int. J. Electrochem. Sci.*, 8 (2013) 10839.